

GoPrune: Accelerated Structured Pruning with $\ell_{2,p}$ -Norm Optimization

Li Xu

School of Mechatronic Engineering and Automation
Shanghai University
Shanghai, China
xljackson@shu.edu.cn

Xianchao Xiu

School of Mechatronic Engineering and Automation
Shanghai University
Shanghai, China
xcxiu@shu.edu.cn

Abstract—Convolutional neural networks (CNNs) suffer from rapidly increasing storage and computational costs as their depth grows, which severely hinders their deployment on resource-constrained edge devices. Pruning is a practical approach for network compression, among which structured pruning is the most effective for inference acceleration. Although existing work has applied the ℓ_p -norm to pruning, it only considers unstructured pruning with $p \in (0, 1)$ and has low computational efficiency. To overcome these limitations, we propose an accelerated structured pruning method called GoPrune. Our method employs the $\ell_{2,p}$ -norm for sparse network learning, where the value of p is extended to $[0, 1)$. Moreover, we develop an efficient optimization algorithm based on the proximal alternating minimization (PAM), and the resulting subproblems enjoy closed-form solutions, thus improving compression efficiency. Experiments on the CIFAR datasets using ResNet and VGG models demonstrate the superior performance of the proposed method in network pruning. Our code is available at <https://github.com/xianchaoxiu/GoPrune>.

Index Terms—Convolutional neural networks, pruning, $\ell_{2,p}$ -norm, proximal alternating minimization, sparse optimization

I. INTRODUCTION

Convolutional neural networks (CNNs) have achieved remarkable success in various computer vision tasks [1], including image classification [2], object detection [3], and semantic segmentation [4]. However, the ever-increasing depth and width of modern CNN architectures have led to substantial computational costs and memory footprints, posing significant challenges for deployment on edge devices such as mobile phones, drones, and robots [5].

During the past few decades, numerous researchers have focused on network compression, including knowledge distillation [6], quantization [7], and pruning [8]. Compared to the former two techniques, network pruning has gained significant attention due to its simplicity and ease of implementation. Unlike unstructured pruning, structured pruning [9] directly discards entire channels, filters, or layers, yielding thinner models that are compatible with off-the-shelf deep learning libraries and general-purpose processors, thereby being more hardware-friendly. Traditional structured pruning methods typically follow a three-stage pipeline: (1) training a full-capacity model, (2) evaluating the importance of layer structures, (3) pruning less-important structures, followed by fine-tuning.

It is worth noting that both structured and unstructured pruning methods revolve around regularization to identify sparse sub-networks. For example, Kumar et al. [10] adopted the ℓ_1 -norm to prune filters and neurons in CNNs, while Kang et al. [11] employed the $\ell_{1/2}$ -norm for individual weights of network pruning and proved its convergence. Recently, Gao et al. [12] applied the ℓ_2 -norm to the selected sub-network and pruned redundant channels in CNNs. Lee et al. [13] utilized the nuclear norm to prune redundant channels in the network. Generally speaking, current regularization-based pruning methods mainly focus on the ℓ_1 -norm or ℓ_2 -norm, while the ℓ_0 -norm [14] is rarely explored. In fact, the ℓ_0 -norm counts the number of non-zero elements, thereby providing a more effective balance between sparsity and performance. Nevertheless, it is an NP-hard problem. Very recently, Ji et al. [15] proposed the ℓ_p -norm and developed an optimization algorithm based on alternating direction method of multipliers (ADMM). Unfortunately, it is an unstructured pruning method and has two shortcomings. On the one hand, the ℓ_p -norm can only take values within the range of $(0, 1)$, excluding the ℓ_0 -norm, which limits the performance [16]. On the other hand, the resulting subproblems require iterative computation, leading to a large computational load. *A natural question then arises: can this method be extended to structural pruning and solve both shortcomings simultaneously?*

In this paper, we propose an accelerated structured pruning framework called GoPrune. Specifically, GoPrune integrates the $\ell_{2,p}$ -norm with $p \in [0, 1)$ into the training objective to induce filter-level sparsity during optimization, enabling the model to learn the importance of each channel automatically. After training, the one-shot channel pruning is performed based on the learned channel importance, followed by a lightweight fine-tuning stage to recover accuracy. Overall, the main contributions can be summarized as follows.

- We propose a novel structured pruning strategy by integrating the $\ell_{2,p}$ -norm with $p \in [0, 1)$, which covers ℓ_p -norm with $p \in (0, 1)$ in [15] as a special case.
- We develop an efficient algorithm with closed-form solutions, which significantly reduces the compression time.
- We verify its superiority through numerical experiments on the CIFAR datasets.

II. METHODOLOGY

A. Notations

In this paper, weight tensors are represented by capital letters. For any $X \in \mathbb{R}^{C_{in} \times C_{out} \times k \times k}$, the j -th channel is denoted by $X_{:,j,:} \in \mathbb{R}^{C_{in} \times k \times k}$ with the corresponding vectorization being $\text{vec}(X_{:,j,:})$. The Frobenius norm is defined as

$$\|X\|_F = \left(\sum_{i=1}^{C_{in}} \sum_{j=1}^{C_{out}} \sum_{m=1}^k \sum_{n=1}^k X_{ijmn}^2 \right)^{1/2}, \quad (1)$$

where X_{ijmn} is the $ijmn$ -th element. For $p \in (0, 1)$, the $\ell_{2,p}$ -norm is defined as

$$\|X\|_{2,p} = \left(\sum_{j=1}^{C_{out}} \|\text{vec}(X_{:,j,:})\|^p \right)^{1/p}. \quad (2)$$

In addition, $\|X\|_{2,0}$ counts the number of non-zero channels. A further notation will be introduced wherever it appears.

B. Model Construction

As stated in [15], different from the ℓ_1 -norm and ℓ_2 -norm, the ℓ_p -norm with $p \in (0, 1)$ can achieve better sparsity and is closer to the ℓ_0 -norm. Assume that $W \in \mathbb{R}^{C_{in} \times C_{out} \times k \times k}$ represents the weights of the neural network and is a four-dimensional tensor. Thus, the loss function is defined as

$$\min_W L(W) + \lambda \|W\|_p^p, \quad (3)$$

where $p \in (0, 1)$ and λ is the parameter to control the sparsity. $L(W) = l(W) + \alpha \|W\|_F^2$, of which $l(W)$ is the cross-entropy loss function and α is the decay weight to prevent overfitting.

Motivated by [17], we leverage the $\ell_{2,p}$ -norm for network pruning and construct

$$\min_W L(W) + \lambda \|W\|_{2,p}^p, \quad (4)$$

where $p \in [0, 1)$. Obviously, it can be regarded as a general case of (3).

C. Optimization

In the following, an efficient optimization algorithm is provided based on the proximal alternating minimization (PAM) technique. By introducing the auxiliary variable $W = U$, (4) can be rewritten as

$$\begin{aligned} \min_{W,U} \quad & L(W) + \lambda \|U\|_{2,p}^p \\ \text{s.t.} \quad & W = U. \end{aligned} \quad (5)$$

The unconstrained version of (5) is

$$\min_{W,U} L(W) + \lambda \|U\|_{2,p}^p + \frac{\beta}{2} \|W - U\|_F^2, \quad (6)$$

where $\beta > 0$ is the penalty parameter. Denote the objective function of (6) as $f(W, U)$. Under the PAM framework, each variable can be updated alternately via

$$\begin{cases} W^{k+1} \in \min_W f(W, U^k) + \frac{\rho_1}{2} \|W - W^k\|_F^2, \\ U^{k+1} \in \min_U f(W^{k+1}, U) + \frac{\rho_2}{2} \|U - U^k\|_F^2, \end{cases} \quad (7)$$

Algorithm 1 Optimization algorithm

Input: $W \in \mathbb{R}^{C_{in} \times C_{out} \times k \times k}$, p , α , λ , β , ρ_1 , ρ_2 , η

Initialize: $k = 0$

While not converged do

1: Update W^{k+1} by (7)

2: Update U^{k+1} by (16)

3: Check convergence: If epoch ≥ 15 , then stop; otherwise $k = k + 1$

End While

Output: W^{k+1} , U^{k+1}

Algorithm 2 Solution of (7)

Input: $W^k, U^k \in \mathbb{R}^{C_{in} \times C_{out} \times k \times k}$, η , β , ρ_1

Initialize: $t = 0$

While not converged do

1: Update $W^{k,t}$ by (10)

2: Check convergence: If $t \geq T_{\max}$, then stop; otherwise $t = t + 1$

End While

Output: W^{k+1}

where $\rho_1, \rho_2 > 0$ and k is the iteration number. The overall scheme is presented in Algorithm 1, and the update rules for W and U are analyzed as follows.

1) *Update W :* The subproblem can be expressed as

$$\min_W L(W) + \frac{\beta}{2} \|W - U^k\|_F^2 + \frac{\rho_1}{2} \|W - W^k\|_F^2. \quad (8)$$

By expanding the norm terms in (8), it can be rewritten in the form of

$$\min_W L(W) + \frac{\beta + \rho_1}{2} \|W - M\|_F^2, \quad (9)$$

where $M = \frac{\beta}{\beta + \rho_1} U^k + \frac{\rho_1}{\beta + \rho_1} W^k$. Recall that $L(W)$ contains the cross-entropy, and there doesn't exist a closed-form solution. Thus, the stochastic gradient descent (SGD) optimizer is applied to each mini-batch. Let t represent the number of iterations and $W^{k,0} = W^k$. It then derives

$$\begin{aligned} W^{k+1} = & W^{k,t-1} - \eta (\nabla_W L(W^{k,t-1})) \\ & + (\beta + \rho_1)(W^{k,t-1} - M) \end{aligned} \quad (10)$$

where ∇_W indicates the gradient of $L(W)$ at W and η is the learning rate. The overall scheme is presented in Algorithm 2.

2) *Update U :* The subproblem can be solved by

$$\min_U \lambda \|U\|_{2,p}^p + \frac{\beta}{2} \|W^{k+1} - U\|_F^2 + \frac{\rho_2}{2} \|U - U^k\|_F^2, \quad (11)$$

which is equivalent to

$$\min_U \lambda \|U\|_{2,p}^p + \frac{\beta + \rho_2}{2} \|U - N\|_F^2, \quad (12)$$

where $N = \frac{\beta}{\beta + \rho_2} W^{k+1} + \frac{\rho_2}{\beta + \rho_2} U^k$. It can be further decomposed into a series of channel optimization problems as

$$\min_{U_{:,j,:}} \lambda \|\text{vec}(U_{:,j,:})\|^p + \frac{\beta + \rho_2}{2} \|\text{vec}(U_{:,j,:}) - \text{vec}(N_{:,j,:})\|^2, \quad (13)$$

where $\text{vec}(U_{:j::})$ and $\text{vec}(N_{:j::})$ are the vectorized forms of $U_{:j::}$ and $N_{:j::}$, respectively. The proximal operator of $\|\cdot\|^p$ is reviewed in the following lemma.

Lemma 1. Consider the proximal operator

$$\begin{aligned} \text{Prox}_{\lambda|\cdot|^p}(a) &= \min_{x \in \mathbb{R}} \lambda|x|^p + \frac{1}{2}(x-a)^2 \\ &= \begin{cases} \{0\}, & |a| < \kappa(\lambda, p), \\ \{0, \text{sgn}(a)c(\lambda, p)\}, & |a| = \kappa(\lambda, p), \\ \{\text{sgn}(a)\varpi_p(|a|)\}, & |a| > \kappa(\lambda, p), \end{cases} \end{aligned} \quad (14)$$

where

$$\begin{aligned} c(\lambda, p) &= (2\lambda(1-p))^{\frac{1}{2-p}} > 0, \\ \kappa(\lambda, p) &= (2-p)\lambda^{\frac{1}{2-p}}(2(1-p))^{\frac{p+1}{p-2}}, \\ \varpi_p(a) &\in \{x \mid x-a + \lambda p \text{sgn}(x)x^{q-1} = 0, x > 0\}. \end{aligned} \quad (15)$$

See [18] for details.

Therefore, the solution of (13) is

$$\text{vec}(U_{:j::}^{k+1}) \in \text{Prox}_{\frac{\lambda}{\rho_2+\beta}|\cdot|^p}(\|\text{vec}(N_{:j::})\|) \frac{N_j}{\|N_j\|} \quad (16)$$

if $\|\text{vec}(N_{:j::})\| \neq 0$ otherwise $\text{vec}(U_{:j::}) = 0$. Afterwards, U^{k+1} can be obtained by rescaling $\text{vec}(U_{:j::}^{k+1})$ into the four-dimensional tensor.

III. EXPERIMENTS

This section first compares the performance of our proposed GoPrune and ADMM [15], then visualizes the compression weight distribution, and finally discusses the effects of p for GoPrune. All experiments are implemented with PyTorch 2.8 and run on a NVIDIA GeForce RTX 4090D.

A. Setups

In the experiments, some ResNet and VGG models are used, including ResNet-20¹, ResNet-50², ResNet-56¹, ResNet-110¹, VGG-16³ and VGG-19³. The selected evaluation datasets are CIFAR-10⁴ and CIFAR-100⁴.

In the compression stage, we set $\rho_1 = \rho_2 = 1.5 \times 10^{-3}$, $\beta = 1.5 \times 10^{-3}$, and $\alpha = 1 \times 10^{-4}$. The weights are compressed towards zero through the PAM over 15 epochs. As for the value of p , for ADMM, $p = 1/5$, and for GoPrune, $p \in \{0, 1/2, 2/3\}$. Let $I_{[c_j]_l}$ represent the importance score of the c_j -th channel in the l -th convolutional layer, which is

$$I_{[c_j]_l} = \frac{|W_{:j::}| - \min(|W_{:j::}|)}{\max(|W_{:j::}|) - \min(|W_{:j::}|)}, \quad (17)$$

where GoPrune performs channel pruning based on this importance score. All models are pruned to a ratio of 0.7, and fine-tuned for 300 epochs.

In addition, two key metrics are considered, i.e., accuracy (ACC) and compression time. To ensure fairness and eliminate

TABLE I: ACC results and compression time (in seconds) on the CIFAR-10 dataset.

Models	TOP-1 ACC (mean±std)		Compression Time	
	ADMM	GoPrune	ADMM	GoPrune
ResNet-20	88.83%±0.10%	89.02%±0.01%	172.56	110.76
ResNet-50	92.14%±0.14%	92.69%±0.13%	651.00	435.18
ResNet-56	90.07%±0.14%	90.23%±0.11%	392.58	219.78
ResNet-110	90.17%±0.12%	90.56%±0.07%	727.80	358.20
VGG-16	91.48%±0.05%	91.87%±0.10%	168.78	108.60
VGG-19	91.24%±0.05%	91.29%±0.04%	213.40	175.38

TABLE II: ACC results and compression time (in seconds) on the CIFAR-100 dataset.

Models	TOP-1 ACC (mean±std)		Compression Time	
	ADMM	GoPrune	ADMM	GoPrune
ResNet-20	60.89%±0.07%	61.10%±0.05%	221.40	145.78
ResNet-50	70.80%±0.08%	70.84%±0.10%	654.00	633.00
ResNet-56	64.54%±0.10%	64.86%±0.05%	413.70	294.00
ResNet-110	65.35%±0.46%	65.61%±0.15%	693.60	502.56
VGG-16	69.24%±0.09%	69.88%±0.07%	164.22	111.78
VGG-19	67.53%±0.07%	67.75%±0.10%	198.00	186.00

differences caused by different initial conditions, the experiments are repeated 35 times, and the results are presented as the mean and standard deviation.

B. Experimental Results

Table I and Table II list the ACC results (mean±std) and compression time (in seconds) of ADMM for unstructured pruning and GoPrune for structured pruning.

It can be concluded that on the CIFAR-10 dataset, GoPrune is comparable to ADMM in terms of accuracy, and even shows some improvement. In terms of compression time, GoPrune significantly outperforms ADMM. Specifically, the average compression time is approximately 1.7 times faster than ADMM, with a compression time speedup of more than 2 times on ResNet-110 and 1.8 times on ResNet-56. This can be attributed to the larger number of parameters and their residual block architectures. Similar conclusions can be drawn on the CIFAR-100 dataset, where the average compression time is improved by 1.3 times.

Overall, compared to the existing ADMM, our GoPrune not only maintains high accuracy and stability but also achieves a significant improvement in compression time.

C. Weights Distribution

This subsection investigates the weight-distribution evolution during the compression procedures. Fig. 1 and Fig. 2 visualize the compressed results of ResNet-50, ResNet-110, VGG-16, and VGG-19 on the CIFAR-10 and CIFAR-100 datasets, respectively. Here, yellow represents the weight distribution after ADMM compression, and blue represents the weight distribution after GoPrune compression. It is clear to

¹<https://github.com/akamaster>

²<https://docs.pytorch.org/vision/stable/models/resnet.html>

³<https://docs.pytorch.org/vision/stable/models/vgg.html>

⁴<https://www.cs.toronto.edu/~kriz/cifar>

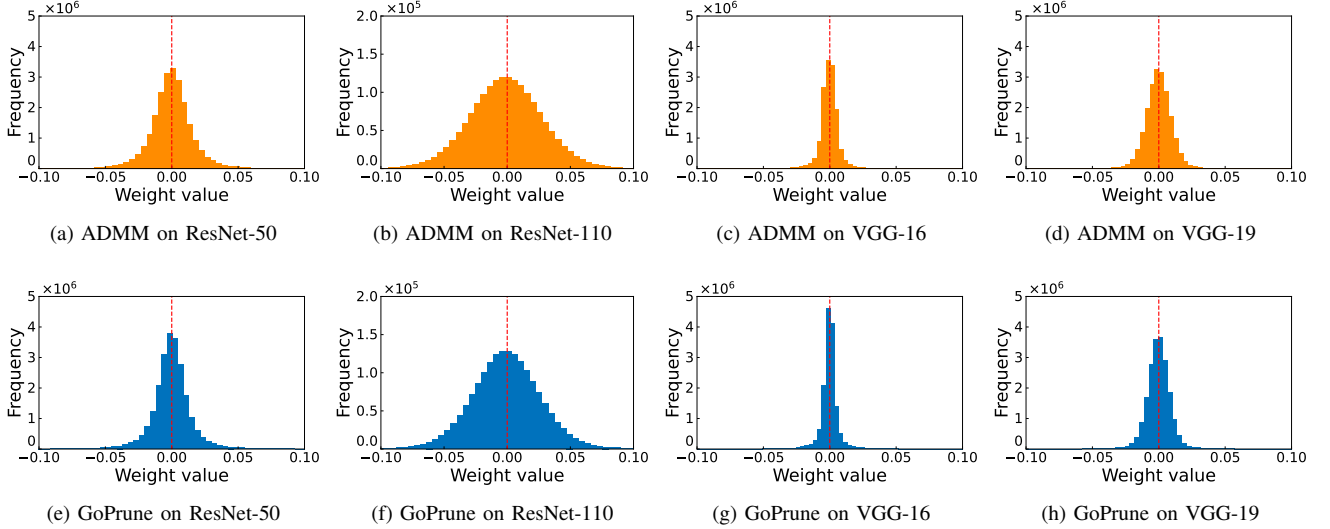


Fig. 1: Weights distribution on the CIFAR-10 dataset.

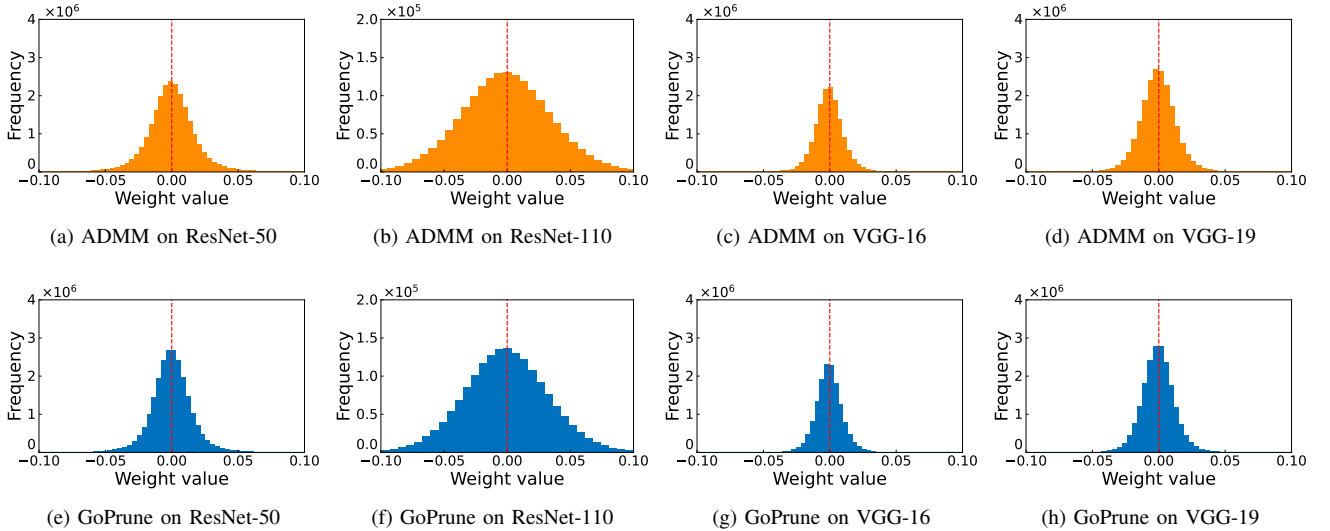


Fig. 2: Weights distribution on the CIFAR-100 dataset.

see that our GoPrune is able to push more weights toward zero compared with ADMM, with the most significant improvement observed on VGG-16 on the CIFAR-10 dataset.

Overall, combined with Subsection III-B, our proposed GoPrune achieves excellent compression efficiency while maintaining high accuracy and less compression time.

D. Effects of p

This subsection discusses the accuracy after compression, pruning, and fine-tuning under three different values of p . Fig. 3 presents the experimental results on the CIFAR-10 dataset. It can be observed that for ResNet-20 and ResNet-50, the best accuracy is achieved when $p = 0$, while for the other models, the highest accuracy occurs at $p = 2/3$. Fig. 4 shows the results on the CIFAR-100 dataset. It can be seen that ResNet-

110 achieves the best accuracy when $p = 1/2$, ResNet-56 performs best when $p = 0$, and the remaining models achieve their highest accuracy at $p = 2/3$.

Overall, the optimal value of p varies across different models and architectures, which validates that extending p from $(0, 1)$ to $[0, 1)$ is of importance.

IV. CONCLUSION

This paper proposes a highly efficient structured pruning framework named GoPrune, which is based on the $\ell_{2,p}$ -norm regularization with $p \in [0, 1)$ and optimized via the PAM algorithm. Unlike the existing ADMM-based ℓ_p -norm unstructured pruning that achieve sparsity only on individual weights, GoPrune calculates the ℓ_2 -norm within each channel and applies the p -norm at the channel level, thereby achieving

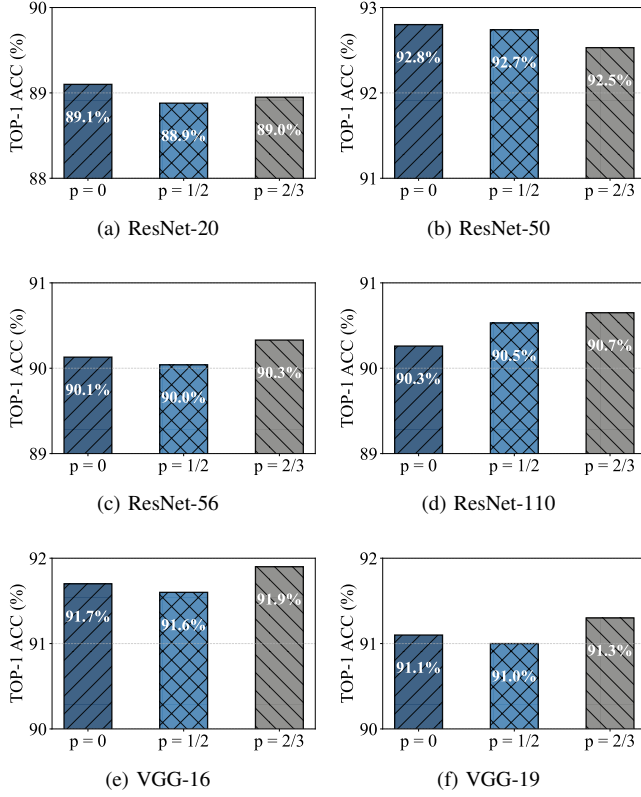


Fig. 3: Effects of p on the CIFAR-10 dataset.

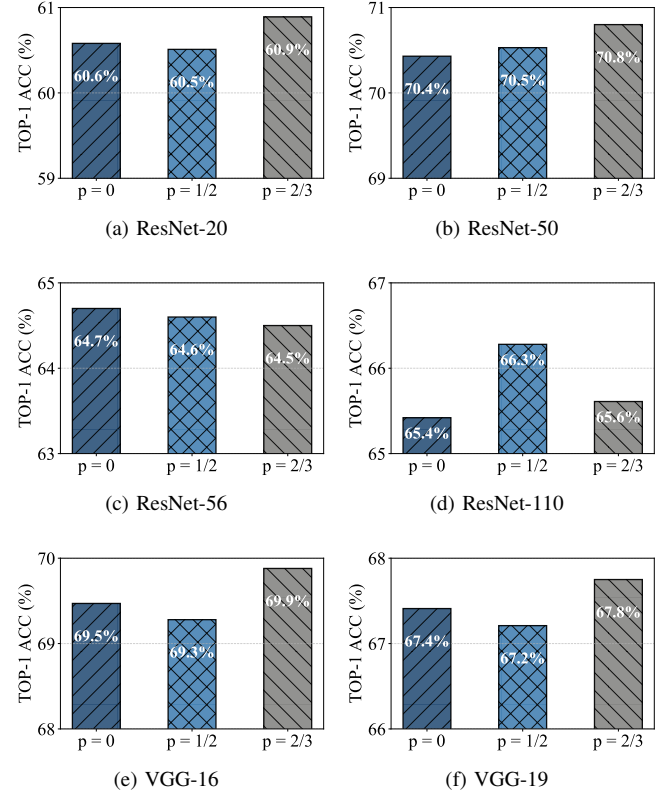


Fig. 4: Effects of p on the CIFAR-100 dataset.

channel-level structured sparsity. Numerical studies validate that our GoPrune outperforms the ADMM-based baseline in both pruning accuracy and compression efficiency.

In the future, we are interested in extending this method to prune large language models.

REFERENCES

- [1] Z. Li, F. Liu, W. Yang, S. Peng, and J. Zhou, "A survey of convolutional neural networks: analysis, applications, and prospects," *IEEE Transactions on Neural Networks and Learning Systems*, vol. 33, no. 12, pp. 6999–7019, 2022.
- [2] B. Xi, Y. Zhang, J. Li, T. Zheng, X. Zhao, H. Xu, C. Xue, Y. Li, and J. Chanussot, "MCTGCL: Mixed CNN-transformer for mars hyperspectral image classification with graph contrastive learning," *IEEE Transactions on Geoscience and Remote Sensing*, vol. 63, pp. 1–14, 2025.
- [3] J. Liu, Y. Han, X. Xiu, J. Zhang, and W. Liu, "Lightweight deep unfolding networks with enhanced robustness for infrared small target detection," *arXiv preprint arXiv:2509.08205*, 2025.
- [4] Z. Chen and Q. Sun, "Weakly-supervised semantic segmentation with image-level labels: from traditional models to foundation models," *ACM Computing Surveys*, vol. 57, no. 5, pp. 1–29, 2025.
- [5] F. Chen, S. Li, J. Han, F. Ren, and Z. Yang, "Review of lightweight deep convolutional neural networks," *Archives of Computational Methods in Engineering*, vol. 31, no. 4, pp. 1915–1937, 2024.
- [6] A. Moslemi, A. Briskina, Z. Dang, and J. Li, "A survey on knowledge distillation: Recent advancements," *Machine Learning with Applications*, vol. 18, p. 100605, 2024.
- [7] B. Rokh, A. Azarpeyvand, and A. Khantemoori, "A comprehensive survey on model quantization for deep neural networks in image classification," *ACM Transactions on Intelligent Systems and Technology*, vol. 14, no. 6, pp. 1–50, 2023.
- [8] H. Cheng, M. Zhang, and J. Q. Shi, "A survey on deep neural network pruning: Taxonomy, comparison, analysis, and recommendations," *IEEE Transactions on Pattern Analysis and Machine Intelligence*, vol. 46, no. 12, pp. 10558–10578, 2024.
- [9] Y. He and L. Xiao, "Structured pruning for deep convolutional neural networks: A survey," *IEEE Transactions on Pattern Analysis and Machine Intelligence*, vol. 46, no. 5, pp. 2900–2919, 2024.
- [10] A. Kumar, A. M. Shaikh, Y. Li, H. Bilal, and B. Yin, "Pruning filters with ℓ_1 -norm and capped ℓ_1 -norm for CNN compression," *Applied Intelligence*, vol. 51, no. 2, pp. 1152–1160, 2021.
- [11] Q. Kang, Q. Fan, J. M. Zurada, and T. Huang, "A pruning algorithm with relaxed conditions for high-order neural networks based on smoothing group $\ell_{1/2}$ regularization and adaptive momentum," *Knowledge-Based Systems*, vol. 257, p. 109858, 2022.
- [12] S. Gao, Z. Zhang, Y. Zhang, F. Huang, and H. Huang, "Structural alignment for network pruning through partial regularization," in *Proceedings of the IEEE/CVF International Conference on Computer Vision*, pp. 17402–17412, 2023.
- [13] D. Lee, E. Lee, and Y. Hwang, "Pruning from scratch via shared pruning module and nuclear norm-based regularization," in *Proceedings of the IEEE/CVF Winter Conference on Applications of Computer Vision*, pp. 1393–1402, 2024.
- [14] F. D. de Resende Oliveira, E. L. O. Batista, and R. Seara, "On the compression of neural networks using ℓ_0 -norm regularization and weight pruning," *Neural Networks*, vol. 171, pp. 343–352, 2024.
- [15] F. Ji, X. Chen, R. Chu, and B. Liu, "Network slimming using ℓ_p ($p < 1$) regularization," *Pattern Recognition*, p. 111711, 2025.
- [16] J. Liu, M. Feng, X. Xiu, and W. Liu, "Towards robust and sparse linear discriminant analysis for image classification," *Pattern Recognition*, vol. 153, p. 110512, 2024.
- [17] X. Xiu, C. Huang, P. Shang, and W. Liu, "Bi-sparse unsupervised feature selection," *IEEE Transactions on Image Processing*, vol. 34, pp. 7407–7421, 2025.
- [18] S. Zhou, X. Xiu, Y. Wang, and D. Peng, "Revisiting L_q ($0 \leq q < 1$) norm regularized optimization," *arXiv preprint arXiv:2306.14394*, 2023.